

## **A ROBUST DRIVER ASSESSMENT METHOD FOR THE BRAIN-COMPUTER INTERFACE**

Ljubo Mercep. *Technische Universität München, Institute for Informatics, Chair for Robotics and Embedded Systems. Boltzmannstraße 3, 85748 Garching bei München.*

Gernot Spiegelberg. *Technische Universität München / Siemens AG. Otto-Hahn-Ring 6, 81739, München, Germany.*

Alois Knoll. *Technische Universität München, Institute for Informatics, Chair for Robotics and Embedded Systems. Boltzmannstraße 3, 85748 Garching bei München.*

### **ABSTRACT**

Brain-computer interfaces (BCI) are a valuable proposition for the long-term vision of the automotive human-machine interfaces and for increasing the personal mobility of users with physical disabilities. In this work, we do not attempt to improve the vehicle control through a BCI. Instead, we focus on assessing the driver's fatigue using a non-invasive BCI technology, a mobile electroencephalograph (EEG). Non-invasive EEG-based approaches for driver assessment often rely on the independent components analysis (ICA) and measure the relative power of specific EEG frequency bands. In the case of wireless and mobile EEG devices, especially outside the domain of medical-grade electronics, a higher number of artifacts and lower channel count can be expected. Main priorities for such devices are ergonomics and usability, with signal quality and robustness on the second place. Such devices significantly simplify experiment design and data collection in automobile simulators and real test-drives. This work presents a robust two-step EEG signal processing method for driver assessment for a consumer-grade EEG BCI, which collects artifact-rich data using a limited number of low-quality saline-pad electrodes. We demonstrate that a reliable assessment of driver state in such conditions is possible, if the independent component analysis is extended through an expert system-based assessment of reliable signal components in a specific region-of-interest on the brain surface. The method additionally eliminates the need for manual artifact removal. We show that the lower sensor count, lower sensor quality and mechanical vibrations can be offset through additional signal processing. We additionally show that the data collected by the BCI provides additional value to the driver assistance, meaning that BCIs can serve both as a human-machine interface and a driver assistance system.

### **KEYWORDS**

Human-machine interface, brain-computer interface, driver assessment, driver assistance.

## 1. INTRODUCTION

The societal impact of a successful and non-intrusive method of reducing the losses in lives and property in traffic accidents is without any doubt large. Depending on the type of the human-machine interface (HMI) used for the primary vehicle control, various methods can be utilized to assess the driver state. In the scope of the automotive research project “Diesel Reloaded“, the brain-computer interface (BCI) is being analyzed as one of the future automotive HMI solutions.

Such interfaces have already been used in semiautonomous and direct vehicle control (Autonomos Labs, 2012). Furthermore, BCI provides personal mobility to physically impeded users, which are not able to operate a standard vehicle equipped with steering wheel and pedals. Even though specific custom-made physical interfaces, one example being miniaturized joysticks, can be used to operate vehicles with only one hand and minimal physical exertion, the BCIs go one step further and read out user’s commands directly at the source. Further development of BCI feedback methods can be expected in the future, but current users have to do away with traditional feedback channels through human senses. It is not our goal to compare the user experience and ergonomics of the current physical interfaces and the BCI. While most drivers could wish to use their vehicles the same way they use their body and insisting on haptic feedback, monitoring their mental state and level of fatigue will remain of high importance.

The BCI provides a clearer insight into the operator’s state, because it additionally captures brain activity not related to the primary task of vehicle control. Lal and Craig (2001) concluded that monitoring EEG may indeed be the most promising method for fatigue detection. Current state of spectral analysis suggests that ratios between the alpha, beta and theta frequency bands can yield acceptable driver classification (Cao, 2010). The currently established methods are however of little use for online assessment of driver state with low-cost consumer-grade EEG input devices in automotive conditions, especially if the user keeps changing head position due to external forces and short glances. We present a two-step method called based on region-of-interest independent component selection for spectral analysis, abbreviated as RISSA for brevity in the rest of the document.

This work is organized as follows. In section 2 we describe the design of the experiment which used to evaluate the approach. In section 3 we present the main properties and issues of analyzed signals captured by the BCI. In section 4 we describe our processing method and the key elements of the contribution. In section 5 we present and discuss the results. Finally, we conclude and present the future work in the section 6.

## 2. EXPERIMENT DESIGN

### 2.1 Driving Simulator

VIRES Virtual Test Drive version 1.1 was used for data collection, complete with an automobile mock-up, a chassis of a Smart automobile, shown in figure 1. A simulation of the driving environment was being shown on a large screen in front of the vehicle mockup. Only one screen was present, hence the possible lack of driver immersion might have affected the results. Furthermore, the simulator was not equipped to provide lateral and longitudinal forces normally experienced during a real test drive. This could have also reflected negatively on the data, but

has to be cross-checked with either a more advanced simulator or a test drive. Simulated vehicle dynamics were comparable to a typical personal automobile.

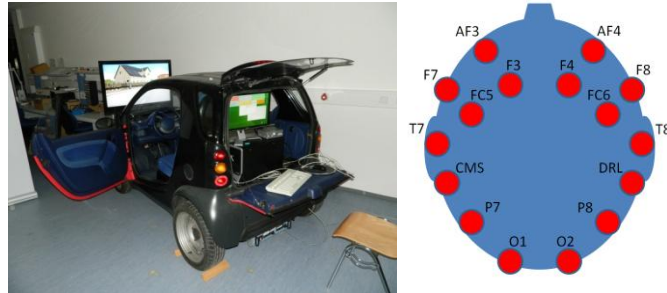


Figure 1. On the left the driving simulator, on the right electrode locations provided by the EEG helm

## 2.2 Brain-Computer interface

A 14-channel wireless EEG helm was used in the experiment. The provided electrodes, after the 10-20 standard, are AF3, AF4, F3, F4, F7, F8, FC5, FC6, P7, P8, T7, T8, O1 and O2. Figure 1 shows the exact electrode location.

The device performs internal super-sampling of the EEG signal with the frequency of 2 kHz and provides the resulting output signal with the frequency of 128 Hz. Effective sampling resolution is 14 bits, with the least significant bit representing  $0.51\mu\text{V}$ . Dynamic range is 8400mVpp. Digital notch filters are active at 50 and 60 Hz. Signal bandwidth in the range of 0.2-45Hz. The helm is using a 2.4GHz wireless band to connect to the personal computer with a wireless dongle, where further data processing takes place. It is powered by a Li-Polymer battery with a theoretical life of 12 hours. Electrodes are of modular design and are equipped with saline sensor pads.

## 2.3 Participants

A total of 21 participants (18 male, 3 female), all in the possession of a driver's license valid in the European Union, took part in the experiment. Mean age was 26.1; the driving license was possessed for a mean duration of 8.2 years. All the participants fall into two groups – the *normal*, which consists of 14 well rested subjects performing the experiment well before 19:00h and the *negative* which consisted of 7 tired participants performing after 19:00h. The subject tiredness was additionally determined through a pre-experiment survey, in which the subjects were asked to provide objective and subjective data regarding their current overall fitness and fitness to operate a vehicle. Personal average sleep time was also compared to the duration of the last sleep. Energy drinks, coffee and similar stimulants were taken into account.

## 2.4 Experiment Course

The entire experiment lasted approximately one hour per participant. At the beginning, the participants were requested to sit in front of a personal computer wearing the EEG helm and try to relax as much as possible for a full minute. They could observe their own EEG activity on the screen during this time. It was not allowed to touch the helm, close the eyes or engage in any form of deep relaxation.

Second phase of the experiment took place in the driving simulator. A simple target following task, not related to driving, was performed with the joystick for 5 minutes. The goal was learning the sensitivity of the device before the driving phase.

Third phase continued inside the simulator, starting with a test drive through a virtual city. After not less than 5 minutes of additional training, the simulation was reset and a 10-minute long data collection was started.

## 3. SIGNAL AND ARTIFACT PROPERTIES

Current approaches for driver state assessment often rely on medical-grade EEG devices with a larger electrode count. The electrodes are often gel based and remain fixed on the scalp. Minor head movement is only partially detrimental to the signal quality. In addition, the electrodes are precisely mounted on the scalp according to the 10-20 standard.

Usage of a helm with a reduced set of saline pad electrodes, which are relatively equally spaced between each other due to the fixed mounting frame, introduces a different set of challenges. The wireless EEG helm is flexible and enables easy fitting, but the electrodes cannot be fixed individually and independently, since they are a part of one rigid unit.

We have observed two types of typical sensor slippage types during the practical work with the EEG helm. The first is an instantaneous contact loss, which is immediately reestablished, which can be called a “shock” artifact. It is characterized by a sudden decrease of measured voltage, a very fast signal jump and a continuation of the decrease until pre-shock signal state is reached. The artifact is usually contained in the time frame of one second.

Another type of slippage manifests as a sudden shift in moving average, which can last for several seconds. These appeared with the subjects with very thick layers of hair directly underneath the electrodes and during strong mechanical vibrations. The upcoming shift in moving average can be detected in advance using the gyroscope built inside the helm, which detects problematic types of mechanical vibration (Mercep, 2013). Vibrations are the largest issue with the used EEG helm. We did not detect electromagnetic interference caused by other electrical devices inside the vehicle. In our case, such devices would be the power electronics and computers running the simulation and located inside the chassis. In a real automobile, these would be infotainment and comfort systems. Such interference could be identified in advance, in the moment when the user requests a certain functionality to be activated, if a connection to underlying vehicle system architecture or all provided human-machine interfaces is present.

Finally, we observed cases of a single electrode permanently not having optimal contact with the scalp. In the worst case, this manifests itself in a signal with no extreme values or extreme slew rates, but neither time-domain samples nor the signal’s spectrum have a biological background. Such data channels can be completely mapped out the collected data for the entire duration of the experiment.

Other artifacts stemming from external sources (such as AC frequency) and various muscle and eye activity are dealt with in the scope of ICA decomposition.

## 4. PROPOSED PROCESSING METHOD

Our proposed approach consists of a pre-experiment preparation phase and an online phase which takes place during the data collection.

### 4.1 Preparation Phase

Let us define a region of interest (ROI) on the brain surface, in which a well-defined set of rules regarding to mapping of brainwave frequency bands and their ratios to driver state exists. In the rest of this document we refer to this set of rules, which is derived from the biological effects of brainwave activity, the biological context table (BCT). It is necessary for the entire ROI to be invariant to the same BCT, which implies that all the relevant frequency bands can be detected throughout the ROI. There can be an arbitrary amount of ROIs with corresponding BCTs on the scalp. In regards to the EEG device capturing the data, they should be weighted by the a priori reliability, based on actual electrode position and density. For the purposes of this work, we have defined one ROI and its BCT in the preparation phase. The focus of this work is placed on the online phase and selecting a reliable independent component inside the ROI. For our experiment, the ROI was set to the frontal and central cortex lobe, mostly due to the higher electrode density for the provided EEG device in this area. Figure 2 shows two independent components in this ROI and presents the building blocks of the signal processing pipeline explained in the following section.

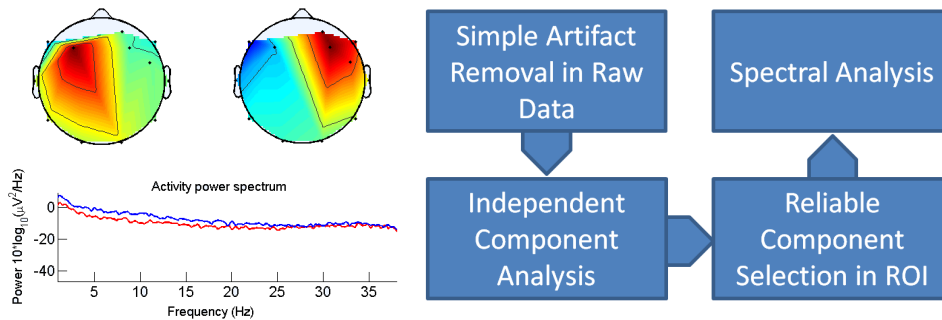


Figure 2. On the left a comparison of power spectrum differences for two ICA components in one ROI, on the right the basic blocks of the signal processing pipeline in the online phase

## 4.2 Online Phase

Once the ROI and appropriate BCT are fixed, we connect the following blocks into the signal processing pipeline:

1. Simple artifact removal in raw data
2. Independent component analysis on the entire scalp
3. Selection of reliable independent component in a ROI
4. Spectral analysis of reliable independent component

The simple artifact removal in step 1 relies on straightforward detection of signal properties already described in section 3 of this work and is not explained further on. In the rest of this section, we briefly touch the methods which were incorporated as-is into our method (such as ICA), and go into detail when describing custom building blocks.

### 4.2.1 Independent Component Analysis

Let the vector

$$s = \{s1(t),s2(t)\dots sn(t)\} \quad (1)$$

contain N independent source signals. Let the vector

$$x = \{x1(t),x2(t)\dots xn(t)\} \quad (2)$$

contain N linear mixtures, which are the result of multiplying the vector of source activity EEG waveforms s by an unknown square matrix A which performed the mixing process, that is

$$x = As \quad (3)$$

The goal is to find the filter which performs the inverse mixing process and enables extraction of the vector u which is a scaled and reordered version of the original vector s. Therefore, it is necessary to find a square matrix W which inverts the mixing the process and produces u

$$u = Wx \quad (4)$$

The main difference between principal component analysis (PCA) and the independent component analysis arises in the assumptions on the nature of differences between s and x. PCA assumes that the data sources are uncorrelated, while ICA has a stronger assumption of statistical independence (Jung, 2001). PCA has been successfully used in the same context of EEG power spectrum analysis (Wu, 2004).The consequence of statistical independence is the factorization of the multivariate probability density function  $f_u(u)$ .

The extended infomax algorithm based on a neural network and proposed by Bell and Sejnowski (1995) is used to find the vector u. The joint entropy  $H(y)$  of the output of a neural processor is maximized in order to minimize the mutual information among the output components  $y_i=g(u_i)$  where  $g(u_i)$  is invertible bounded nonlinearity. The algorithm separates sources with both supergaussian and subgaussian distributions. In this work, the number of independent components has been set to the number of active EEG channels per experiment. This was not always the total number of electrodes (14), due to the rejection of bad EEG channels.

#### 4.2.2 Selection of Reliable Independent Component in a ROI

The ICA components in ROI are evaluated with an expert-based belief network, which provides a measure of so-called goodness for every independent component. We always selected the component with the maximal goodness for the next step, the spectral analysis.

Main contributing factors to the component goodness are:

1. Number of electrodes in the vicinity of the component
2. Simple artifacts' amount from the electrodes near to the component
3. Dipole properties of the independent component
4. Spread of the component over the frontal areas prone to facial muscle artifacts

Most of the factors were derived from the existing and well-defined rules for manual component identification when using ICA with common signal toolboxes, such as EEGLAB from the Swartz Center for Computational Neuroscience.

A Bayes belief network  $N$  contain the contributing factors is shown on the figure 3. This network can be extended in the scope of future work to take as many factors into account as possible. Using the built-in gyroscopic sensors for detection of head movement and correlating these movements to a map of electrodes with different sensitivity to different kinds of head motion is a good example. The inference complexity is not an issue, since the network size is negligible. For the future expansion, we suggest using the more performing exact-inference method called the junction tree in this step, since we assume that the number of rules and the resulting network will rapidly grow. The goal is to keep the method online while running on embedded hardware. This suggestion does not constitute a part of the scientific contribution of this work, but rather represents a method for the efficient implementation of RISSA.

Let us briefly describe the junction tree-based inference.

Let  $J$  be a subgraph of the clique tree  $C$ .  $J$  is a junction tree iff:

1.  $J$  is a tree
2.  $J$  contains all the nodes of the clique graph  $C$
3. For each pair of cliques  $C_1$  and  $C_2$  which have an intersection  $S$ , all cliques on the path between  $C_1$  and  $C_2$  also contain  $S$ .

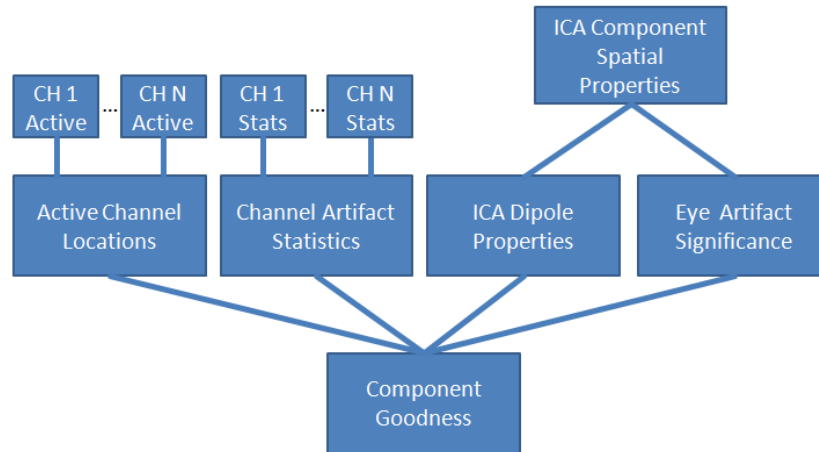


Figure 3. Belief network used for component evaluation

The benefits of a junction tree, as compared to the original Bayesian network, are:

1. Frequent updates of clique probability tables incurred by dynamic artifact detection are performed more efficiently
2. Querying the network is optimized for a desired set of often asked questions
3. The junction tree is pre-constructed before the experiment and does not change structurally during the data acquisition
4. New nodes are easily added to the original belief network and integrated into the junction tree before the experiment

Drawing a parallel to the techniques used in dynamic programming, a junction tree can be seen as cache of subjoint probabilities used during the variable elimination. Probabilities are update by a message-passing algorithm, which is currently the most efficient exact reference method for concurrently computing multiple queries (Pan, 1997). However, the running time is exponential in the size of the largest clique.

Previously introduced region of interest (ROI) can contain multiple instances of spatially localized ICA components. The independent component with the largest goodness is selected for the analysis. To recap, frontal and central cortex area was chosen as the region-of-interest, due to the highest electrode density.

#### 4.2.3 Spectral Analysis of the Reliable Component in ROI

Our spectral analysis relies on the set of rules inside the previously defined biological context table (BCT). Cao (2010) found that the band power of  $\theta$ ,  $\alpha$  and  $\beta$  waves reflect the difference in driver vigilance in different ways, based on the observed cortical area. In the central cortex, the  $\theta$  band was stronger in the sleepy state. In the frontal cortex, the  $\beta$  band was weaker in the sleepy state. The  $\alpha$  band was only significant for classification in the occipital and parietal cortex. However, we have found a significant difference in the frontal and central cortex activity by measuring the ratio  $\beta/(\theta+\alpha)$ , where  $\alpha$  contains both slow and fast alpha waves. Due to the large number of artifacts at frequencies lower than 4 Hz, we avoided analyzing the  $\delta$  band, even

though it was found to be significant for the frontal cortex. As the end result, our BCT for the ROI of interest was set to the ratio  $\beta/(\theta+\alpha)$ .

## 5. RESULTS

A single 30-second long sample was taken in the default state, while the user was not performing any activity. Six 30-second long samples were taken in the second phase in the driving simulator, while the user was driving through the virtual city. With this data, we benchmarked two aspects of our signal processing method.

Firstly, the effectiveness of the belief network used for component selection was evaluated, in comparison to the choices made by manual data inspection. These results are shown in the table 1.

Table 1. Accuracy of the independent component selection in the region of interest

ICA Components in ROI	Experiment Phase	
	Default Activity	Driving
Mean Number of Alternatives	4.14	4.26
First Choice Selection Rate	93%	91%
Second Choice Selection Rate	100%	100%

We can observe that the ICA mapped an average of 4 components inside our region of interest during both phases. The method correctly identified the most suitable component with the accuracy larger than 90% in both phases. The second choice selection rate describes how often the best component received the second best goodness i.e. how often the method made a mistake of placing the correct component on the second best place. It is clear that when the method fails to select the very best component (>10% of the cases), it always places that component on the second place. The difference between the two after spectral analysis is often minimal, so this does not affect the following part of result analysis.

Secondly, we analyzed the actual difference between the fatigue assessments of the two driver groups as provided by the BCT in the defined ROI. Each group received a scalar value of the frequency band ratio. A two-sample t-test has been performed on the ratios for both test groups. As the result, the null hypothesis has been rejected with the significance level of 5%, meaning that the two groups do exhibit a statistically significant difference. These results are presented in the table 2.

Table 2. Differences in ratio  $\beta/(\theta+\alpha)$  between two driver groups

Experiment Phase	Test Group	
	Normal	Negative
Default Brainwave Activity	0.8898	0.7185
Driving in the Simulator	0.8292	0.7027

The collected data summarized in both tables confirms that the independent components are being correctly identified and that the BCT in the selected ROI correctly identified the driver state during our experiment. As a result, we claim that the RISSA approach is robust enough to justify further development and experiments in real-life conditions.

## 6. CONCLUSION AND FUTURE WORK

We have demonstrated how consumer-grade BCIs can be deployed in automobiles to assess the driver fatigue. The issues of low-quality electrodes and low electrode count were alleviated with additional signal processing effort. Our contribution has both increased the robustness of the established methods for EEG signal processing and extended the usefulness of consumer electronics BCI devices in the automotive area for the purpose of driver state detection. One important question is how the resulting driver assessment can be meaningfully used for increasing traffic safety.

We suggest a practical approach based on influencing the driver state through infotainment and/or comfort systems, in an attempt to bring the driver back into an alerted and wake state. One option, already made possible in our experiment vehicle, is manipulating the ambient lighting of the driver's workspace. Sudden change of ambient color or a shift to daytime color temperatures can affect the driver wakefulness. Another option is alerting the driver with visual and audio cues, some of which require user interaction to be reset again. Some examples are illustrated in figures 4 and 5.

As the last step of future work, the method could be tested inside our sidestick<sup>1</sup>-operated drive-by-wire prototype, the Innotruck. The RISSA can be integrated into a combined human-machine interface and driver assistance module, since it provides fatigue information (attributed to classical driver assistance devices), while relying on large amounts of raw data from the HMI.

---

<sup>1</sup> Sidesticks in the Innotruck are two spherical input devices with one degree of freedom (left-right) and two buttons for throttle and braking, vaguely resembling a joystick.



Figure 4. The EEG helm can be comfortably worn while the prototype vehicle is driven with conventional human-machine interfaces (Image by Juan Jose Gonzalez Herrero)



Figure 5. The Innotruck experimental vehicle of the project Diesel Reloaded is equipped with controllable LED ambient lighting, shown here while illuminating driver's workplace in blue

## ACKNOWLEDGEMENT

We would like to thank the International Graduate School of Science and Engineering (IGSSE) as well the Institute of Advanced Study (IAS) of the Technische Universität München for all the support in the organization of our project. Furthermore, we would like to thank fortiss, an Institut der Technischen Universität München, for all the constructive advice and practical support.

## REFERENCES

- Bell, A. J. and Sejnowski, T. J., 1995. A non-linear information maximization algorithm that performs blind separation, *Advances in Neural Information Processing Systems*, 7, pp. 467-474.
- Brain Driver 2012, AutoNOMOS labs Videos, Berlin, online video, accessed 15 November 2012, <<http://www.autonomos.inf.fu-berlin.de/media/videos>>.
- Cao, L. et al, 2010. EEG-based vigilance analysis by using fisher score and PCA algorithm, *Progress in Informatics and Computing (PIC)*, 2010 IEEE International Conference on , vol.1, pp. 175-179
- Jung, T. and Makeig, S., 1994. Estimating Level of Alertness from EEG, *Proceedings of the 16th Annual International Conference of the IEEE Engineering in Medicine and Biology Society*, 1103-4, 1994
- Jung, T. et al, 2001. Analysis and Visualization of Single-Trial Event-Related Potentials, *Human Brain Mapping*, vol. 14, pp.166-185
- Lal, S.K.L. and Craig, A., 2001. A critical review of the psychophysiology of driver fatigue, *Biological Psychology*, Volume 55, Issue 3, pp. 173-194
- Mercep, Lj., Spiegelberg, G. and Knoll, A. 2013. Reducing the impact of vibration artifacts in a brain-computer interface using gyroscope data. *In IEEE Eurocon 2013*, Zagreb, Croatia.
- Pan, H. et al, 1997. Information Fusion, Causal Probabilistic Network And Probanet II: Inference Algorithms and Probanet System, *Proc. 1st Intl. Workshop on Image Analysis and Information Fusion*, pp. 445-458
- Wu, R. et al, 2004. Estimating driving performance based on EEG spectrum and fuzzy neural network, *Neural Networks, Proceedings*, vol.1, no., pp. 4 vol. (xlvii+3302)